TESLA-Report 1994-31

DAPNIA/94-10

TESLA Final Focus System with Superconducting Magnets in the Interaction Region: Optics, Tolerances and Magnet Design.

Olivier NAPOLY, Etienne KLEIN
DAPNIA/SEA
and
Jean Michel RIFFLET
DAPNIA/STCM

CEA, DSM/DAPNIA, CE Saclay, 91191 Gif/Yvette CEDEX

ABSTRACT

The TESLA final focus system is presented for a centre of mass energy of 500 GeV and $1000 \times 64 nm^2$ beam sizes at the IP. The effect of magnets misalignment and field errors is analyzed using the recently available program FFADA, and the consequence of ground motion on the system is studied. A design for the last doublet superconducting quadrupoles, based on the LHC quadrupoles, is proposed. Tolerances to higher multipole components in the last doublet are analyzed as well as the effect of the main solenoid. A scheme for beam separation, based on existing electrostatic separators, is investigated.

19 December 1994

1 Introduction

The basic idea of the TESLA design for 500 GeV centre of mass energy is that the high luminosity is obtained with moderate beam spot sizes at the interaction point (IP), as compared with other linear collider designs, and with a very high beam current. Hence the beta-functions at the IP are larger than in any other designs. This together with the expected 10^{-3} relative energy definition of the beam, eases the design of the final focus optics. This advantage is balanced by the difficulty to clear the spent beam power and the secondary background (photons from synchrotron radiation and beamstrahlung, electron-positron pairs and hadrons). It is also used to offer a 6 meter long free space around the IP to design the detector and the interaction region.

Another specific property of TESLA is the large 1 μs separation of the bunches. It opens the possibility to collide the beams head-on and to separate them outside of the interaction region. In order to clear all the debris of the collision on axis through the interaction region, it is then necessary to use superconducting magnets with large enough aperture and gradient. If iron-free, these magnets can operate in the field of the detector solenoid and therefore need not be shielded by compensating solenoids. This allows a significant reduction in transverse dimension and weight.

We present a version of the TESLA final focus system adapted to the latest set of beam parameters for 500 GeV centre of mass energy (Sect.2). This new version obeys the same general principles as the preceding one [1]. Its optics has been derived and its properties analyzed by using the program FFADA [2]. Its length has been reduced down to 370 m (Sect.3). The total bandwidth, of the order of 1.7%, has been obtained by optimizing the beam demagnifications achieved by the first and by the final telescope. According to tracking simulations (Sect.4) the luminosity shows no degradation for Gaussian relative energy spreads up to 3×10^{-3}. The calculation of the incoming beam and outgoing synchrotron radiation envelopes (Sect.5) indicates that clearing the synchrotron radiation through the last doublet requires beam transverse collimation of $12\sigma_x$ and $38\sigma_y$. The effects of beam mismatch at the IP and of magnet misalignment and field errors are analyzed in detail (Sect.6). Comparison with a ground vibration spectrum recently measured at CERN [3] suggests that the vertical vibrations of the magnets, *including the last doublet ones*, can be corrected with a feedback system based on the 10 Hz beam repetition rate with less that 2% luminosity loss.

A design for the superconducting magnets of the last doublet is proposed (sect.7). It is based on the LHC magnet prototypes [4] which reached 250 T/m with a physical aperture diameter of 48 mm. According to this design, the outer diameter of a cryostat containing the doublet is 442 mm for a total weight of about 1 ton. Finally, a beam separation scheme is considered. It is based on existing 4 m long electrostatic separators [5] with 3 MV/m field and 10 cm gap, compensated by a weak magnetic field in such a way that the incoming beam is not bent. The outgoing beam can be deflected after 64 m by an angle of 1.5 mrd and a horizontal separation of 5 cm which guarantees that the beam-beam kick is negligible These separators would be located in front of the last doublet.

2 The Beam Parameters

The beam parameters for 500 GeV cm energy version of TESLA are as follows:

Energy	[GeV]	:	250.
Horizontal RMS at the IP	[nm]	:	1000.
Vertical RMS at the IP	[nm]	:	64.
Horizontal normalized emittance	[m]	:	2.0e-5
Vertical normalized emittance	[m]	:	1.0e-6
Longitudinal RMS	[mm]	:	1.0
Relative energy RMS		:	1.e-3
Bunch population		:	5.0e+10
Repetition rate	[Hz]	:	8.0e+3

With these parameters, the values of the beta-functions at the interaction point (IP) are:

$$\begin{aligned} \beta_x^* &= 24.5\,\text{mm} \\ \beta_y^* &= 2.0\,\text{mm} \end{aligned} \tag{1}$$

The expected luminosity including the "hour glass" reduction factor $H_A = 0.949$ but without the pinch enhancement factor is $\mathcal{L} = 2.36 \times 10^{33}\text{cm}^{-2}\text{s}^{-1}$.

3 The Optics Layout and the Momentum Bandwidth

The optics and hardware parameters for the upgraded version of the TESLA final focus system (FFS) are listed below :

Input parameters for FFS

Total length of the FFS		[m]	:	370.
Total horizontal demagnification			:	68.1
Total vertical demagnification			:	98.6
Parameters of Final Telescope				
Horizontal FT demagnification	XM = -R22		:	8.
Vertical FT demagnification	YM = -R44		:	30.
Length of last drift		[m]	:	3.0
Length of last but one drift		[m]	:	0.35
Length of last quadrupole	D	[m]	:	1.92
Length of last but one quadrupole	F	[m]	:	1.27
Pole-tip field of last doublet quads		[T]	:	6.
Aperture diameter of last doublet quads		[mm]	:	48.
Parameters of Matching Telescope				
Length of last quadrupole	D	[m]	:	0.55
Length of last but one quadrupole	F	[m]	:	0.33
Maximum pole-tip field		[T]	:	1.4
Aperture diameter of last doublet quads		[mm]	:	2.

These parameters have been used as input or calculated by the program FFADA [2] to derive the optics

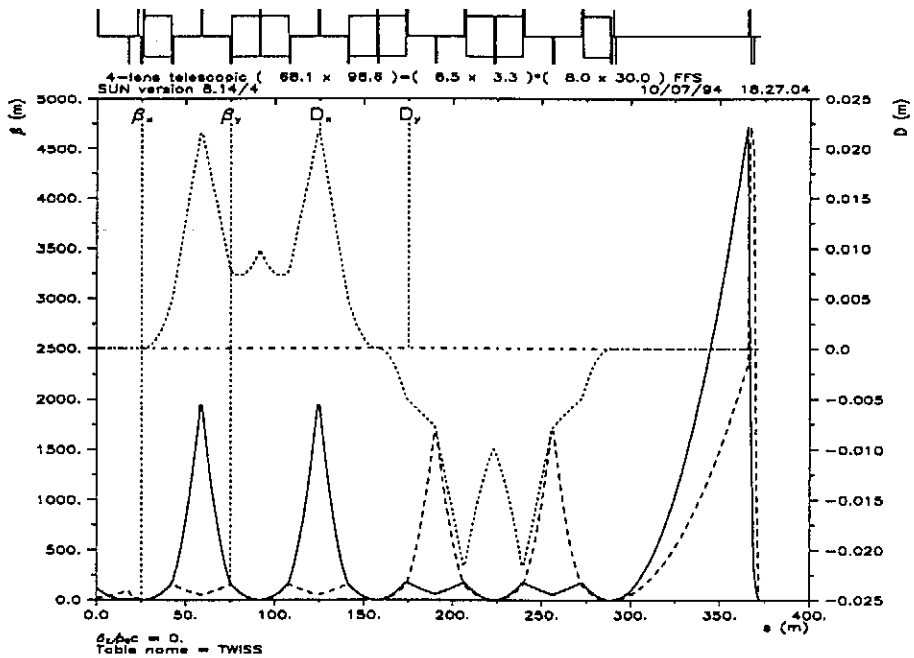

Figure 1: Lattice layout and orbit functions of the FFS.

of the FFS and analyze its properties. The corresponding lattice layout and optics functions, calculated with MAD [6], are shown in Fig.1

The demagnifications assume input beta-functions

$$\begin{aligned} \beta_x &= 113.5\,\mathrm{m} \\ \beta_y &= 19.5\,\mathrm{m} \end{aligned} \tag{2}$$

corresponding to a 90° FODO period of 66.5 m at the end of the linac. The total length has been reduced from 600 m in [1] to 370 m without too much degradation of the chromatic bandwidth of the system. The dependence of the horizontal and vertical beta-functions at the IP on the relative energy difference $\delta = (E - E_0)/E_0$ is plotted in Fig.2 . The momentum bandwidth estimated from the doubling of the horizontal beta-function is ± 0.9 %. Further reduction of the total length induces a rapid degradation of this bandwidth.

The complete beam line is described, in the MAD format, in Appendix A.

4 Tracking Simulations

Two bunches of 5,000 macro-particles with 0.1% Gaussian rms energy spread have been tracked, with MAD and also with DIMAD [7] through the FFS beam line at the 2nd order with synchrotron radiation effects. With both programs, the luminosity calculated, with no pinch effect, from the output beam distributions is $\mathcal{L} = 2.3 \times 10^{33}\mathrm{cm}^{-2}\mathrm{s}^{-1}$.

In order to complete the chromatic analysis of the FFS, Fig. 3 shows the evolution of the relative spot sizes and the luminosity when increasing the rms energy spread of bunches with Gaussian energy distributions (nót truncated). It shows that the luminosity is not degraded up to 3 per mil Gaussian energy spread . It also confirms, after Fig.2, that the energy acceptance is limited by the blow up of the horizontal spot size.

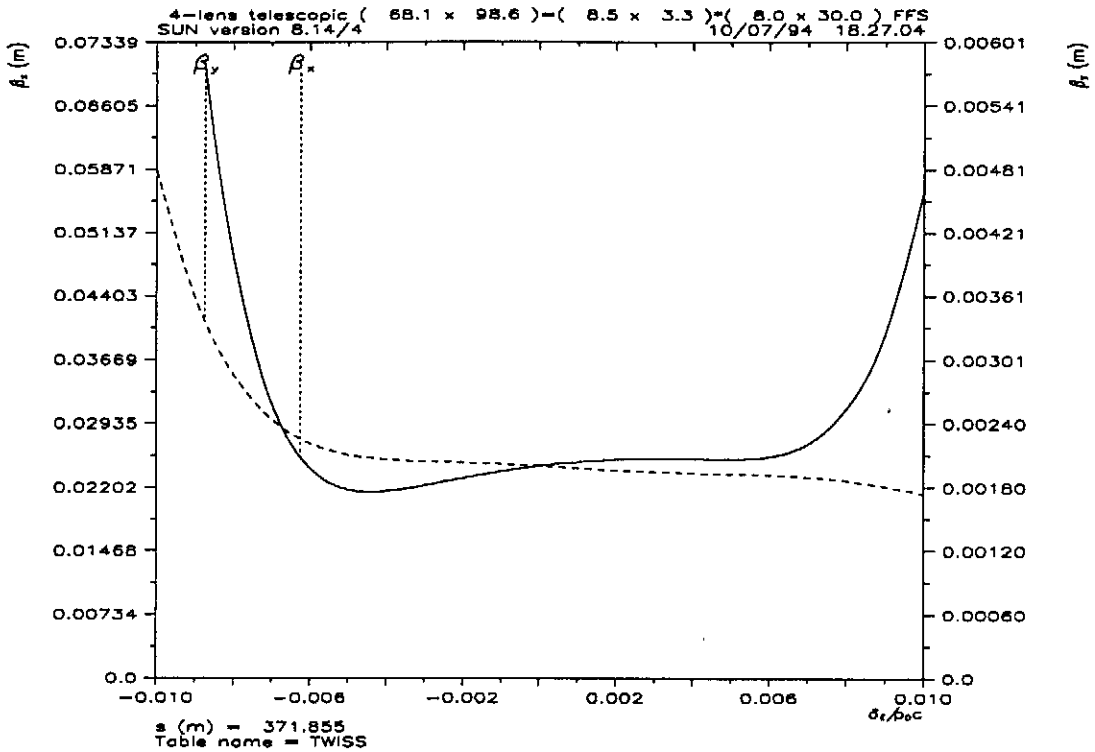

Figure 2: Energy dependence of the Twiss beta-functions at the IP.

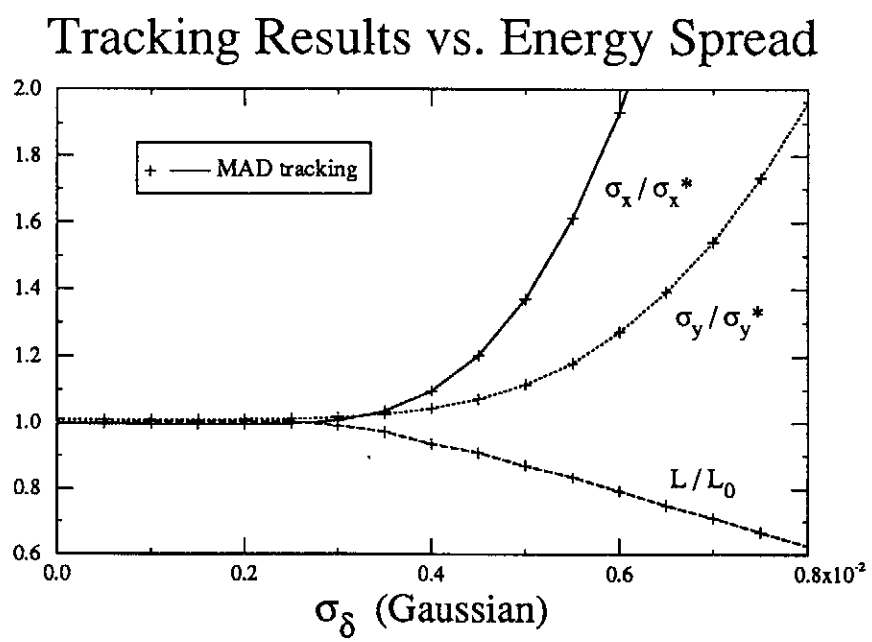

Figure 3: Dependence of the spot sizes and luminosity on the Gaussian rms relative energy spread.

5 The Beam Envelopes and Synchrotron Radiation in the Last Doublet

The DBLT module of FFADA calculates the Twiss α and β functions (Fig.4), the envelopes of

the incoming beam (Fig.5) and of the synchrotron radiation photons in the two opposing doublets. The

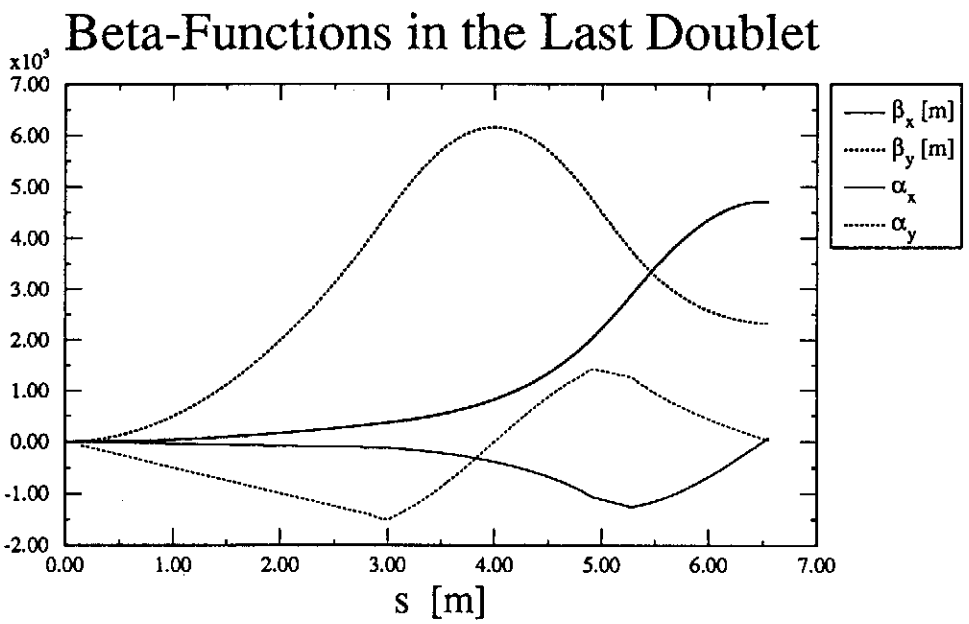

Figure 4: Twiss functions in last doublet (the IP is at s=0).

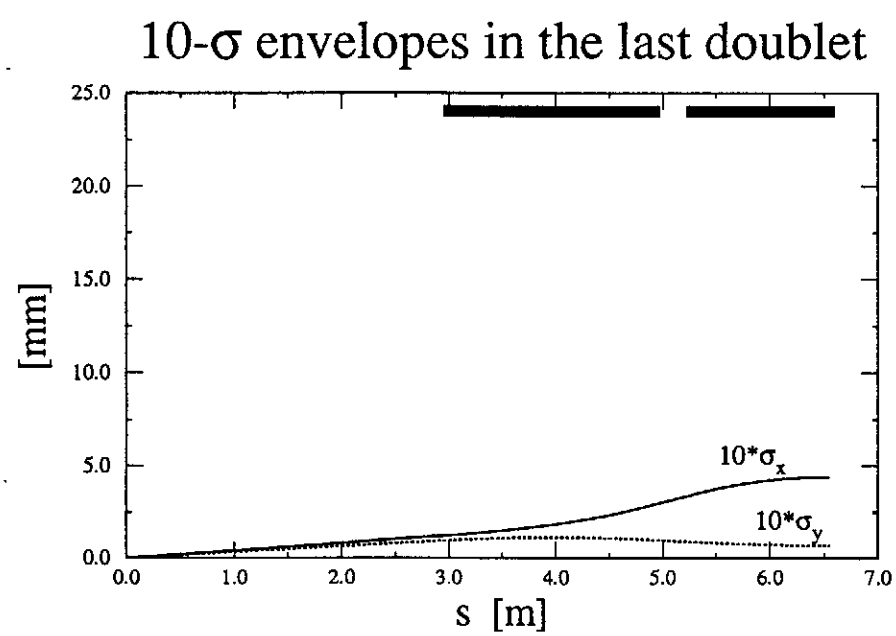

Figure 5: 10-σ envelopes of the incoming beam in the last doublet aperture (the IP is at s=0). The pole-tip aperture of the quadrupoles is represented by the thick lines.

requirement that no photon hit the circular exit aperture of the quadrupoles (see Fig.6) leads to the transverse collimation of the incoming beam at 11.9-σ_x and 38.7-σ_y. As shown in Fig.7, the collimation requirements coming for clearing the vertex detector at the IP, assuming a 30 mm diameter aperture, are less stringent.

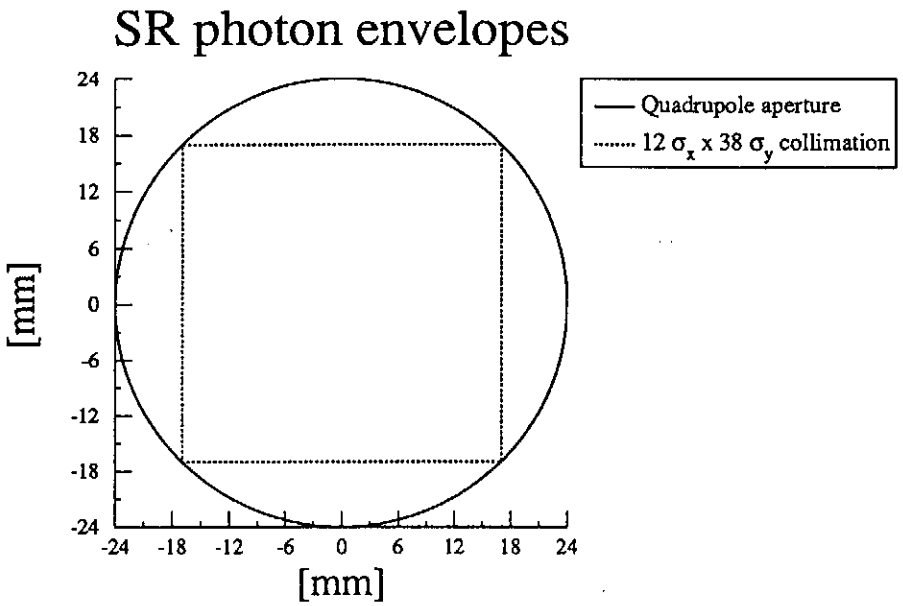

Figure 6: Photon beam boundary in the 48 mm exit aperture of the superconducting quadrupole.

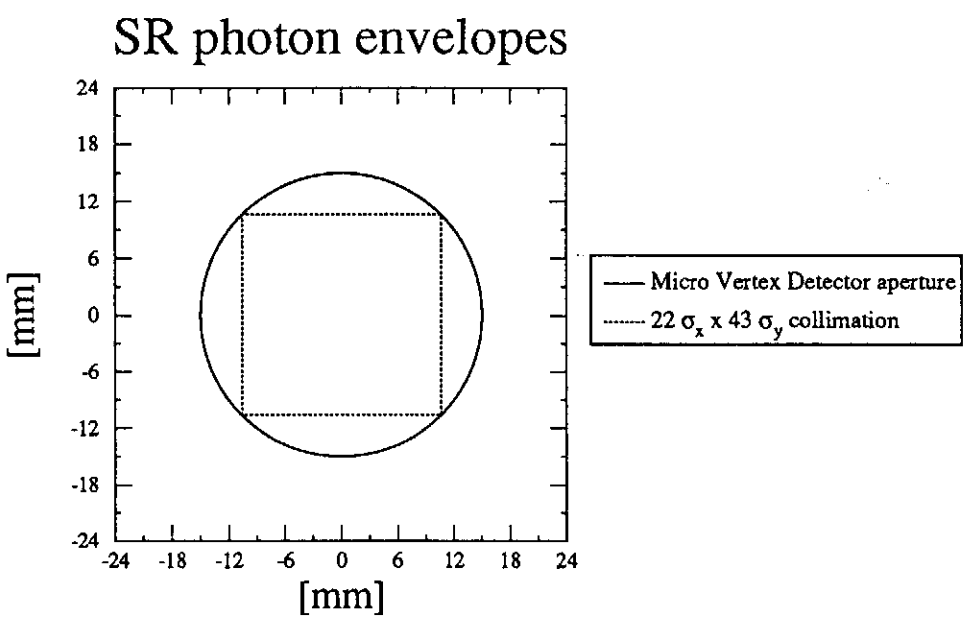

Figure 7: Photon beam boundary in the 30 mm aperture of a vertex detector.

The beam size limit arising from the synchrotron radiation in the last quadrupoles (the so-called "Oide effect") is calculated from the theoretical predictions [8] and from the tracking simulations with MAD and DIMAD. The results, for the 48 mm aperture magnets, are plotted in Fig.8 for the horizontal beam size and in Fig.9 for the vertical one. The nominal spot sizes of 1000×64 nm^2 are safe from this effect for the emittances considered.

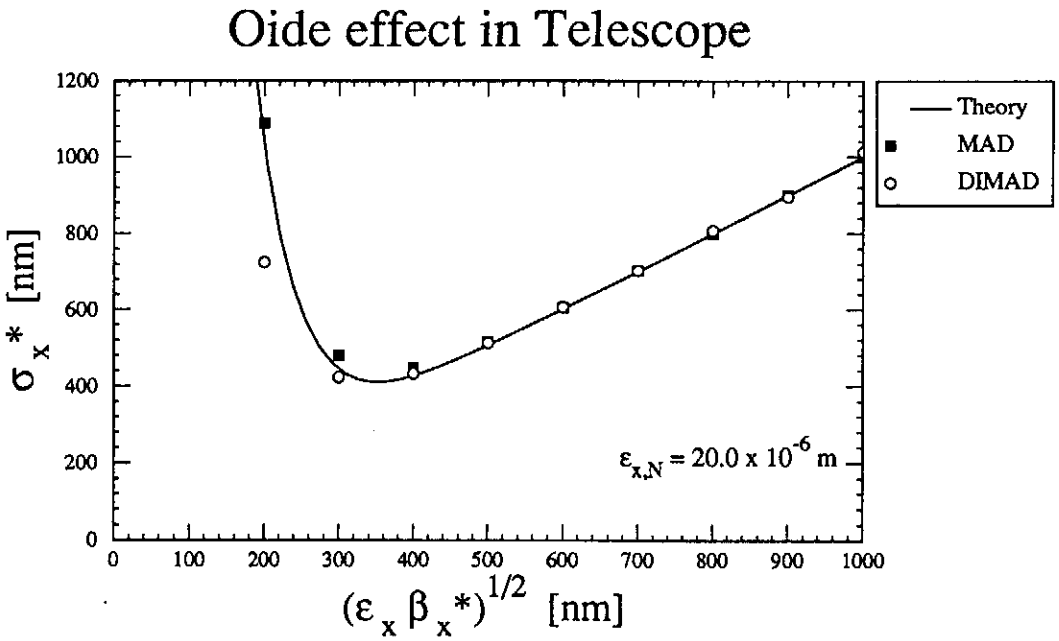

Figure 8: Oide effect in the horizontal plane.

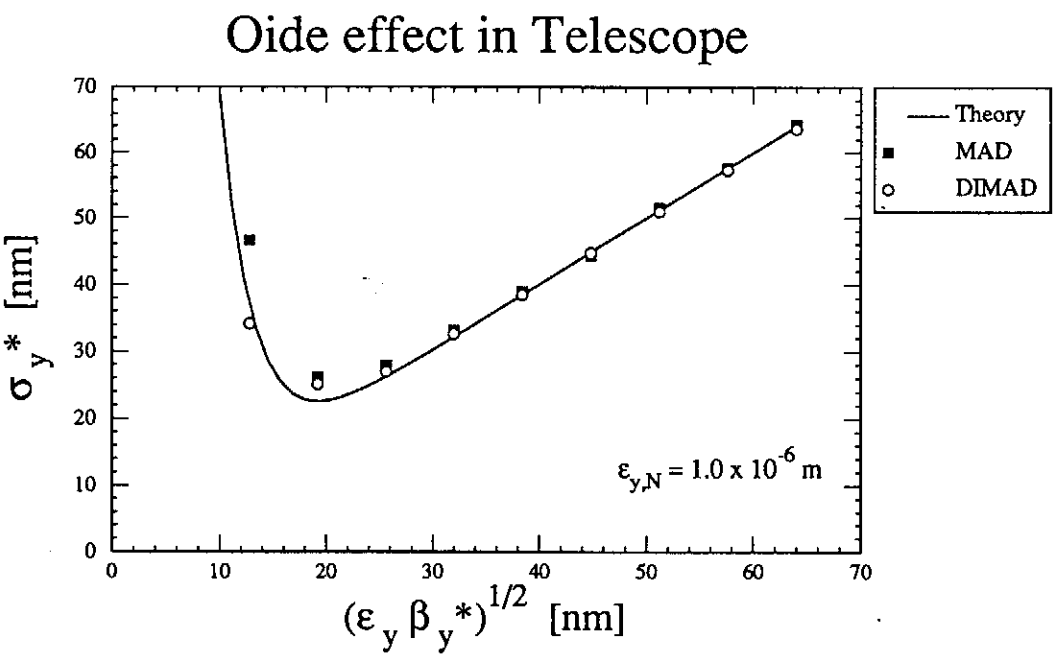

Figure 9: Oide effect in the vertical plane.

The detailed output from the DBLT module calculations is given in Appendix B.

6 Error Analysis

6.1 Luminosity loss from beam offset and dispersion at the IP

The DIFFLUM module of FFADA calculates the luminosity expected from the beam parameters at the IP, assuming no pinch forces. Since, for head-on collisions, the luminosity is at a maximum with

respect to horizontal and vertical beam offsets, crossing-angles and dispersions, the program calculates the second derivatives [9] of the luminosity with respect to the preceding quantities. The complete results from DIFFLUM for the TESLA parameters assuming a Gaussian energy distribution of 0.1% relative rms, are given in Appendix C.

6.2 Magnet misalignment and field errors

The error and tolerance analysis is performed by the module ERROR of FFADA. The isolated effect of misalignment and field errors of each quadrupole and sextupole of the FFS is first considered (the errors affecting dipoles have not been studied yet). The *linear* derivatives of the 0^{th} order (central trajectory) and 1^{st} order (transfer matrix) FFS transfer map are calculated with respect to each type of magnet errors, namely: the **6-dimensional displacements** of quadrupoles and sextupoles, and the **gradient error** of quadrupoles. Most of these results are presented in a series of bar plots which we describe below. The effect of errors affecting the transfer map at the 2^{nd} and higher orders, like typically sextupolar errors, have not yet been considered and will be included in a later version of FFADA.

The number of magnets of each type in the FFS is summarized in the first output of the ERROR module, given in Appendix D.

6.2.1 Transverse displacements

A horizontal or vertical displacement of a **quadrupole** creates:

- at 0^{th} order:
  - a horizontal or vertical position offset of the central trajectory at the IP (see Fig.10) ;
  - a horizontal or vertical angular offset of the central trajectory at the IP.
- at 1^{st} order:
  - a horizontal or vertical dispersion at the IP (see Fig.11) ;
  - a horizontal or vertical angular dispersion at the IP ;
  - a normal (for horizontal) or skew (for vertical) quadrupole gradient error, generated by the horizontal or vertical position and angular offset of the central trajectory in the downstream sextupoles. Since the sextupoles come by pair separated by $-\mathbf{1}$ transfer matrix, these gradient errors cancel for all quadrupoles located outside of the two sextupole-pairs. The normal gradient errors lead to a longitudinal shift δz^* of waist of the horizontal and vertical beta-functions at the IP (see Fig.12). The skew gradient errors lead to xy-coupling at the IP (see Fig.13).

A horizontal or vertical displacement of a **sextupole** creates (at the linear order in the displacement):

- at 1^{st} order:
  - a horizontal or vertical dispersion at the IP (see Fig.11) ;
  - a horizontal or vertical angular dispersion at the IP ;
  - a normal (for horizontal) or skew (for vertical) quadrupole gradient error. Like above, the normal gradient errors induce a longitudinal shift δz^* of the horizontal and vertical β–waists at the IP (see Fig.12), and the skew gradient errors lead to xy-coupling at the IP (see Fig.13).

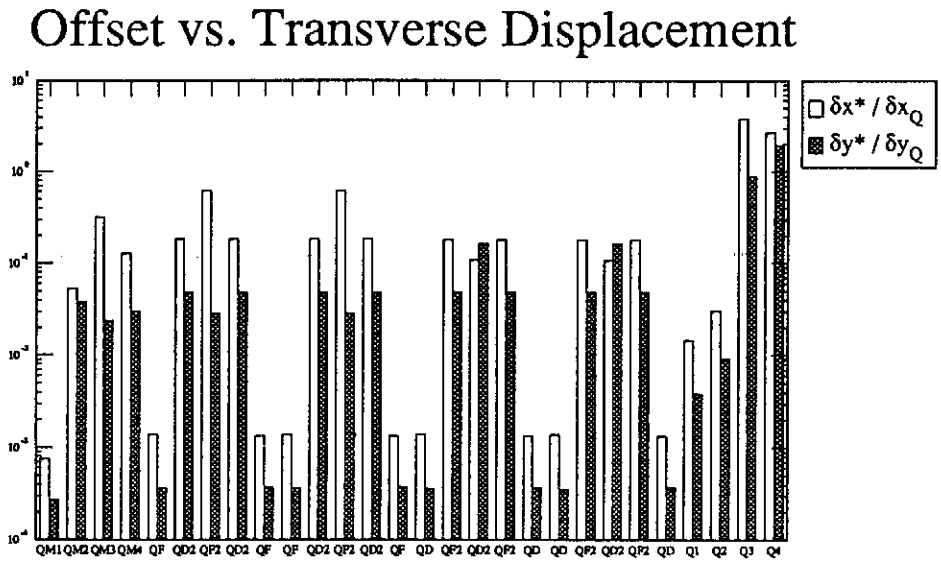

Figure 10: Ratio of IP offset to quadrupole transverse displacement.

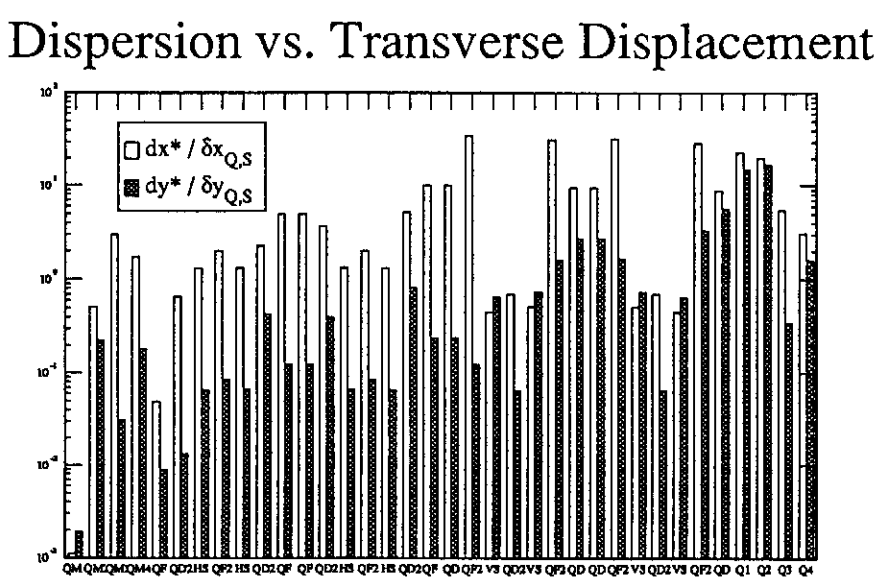

Figure 11: Ratio of IP dispersion to quadrupole and sextupole transverse displacement.

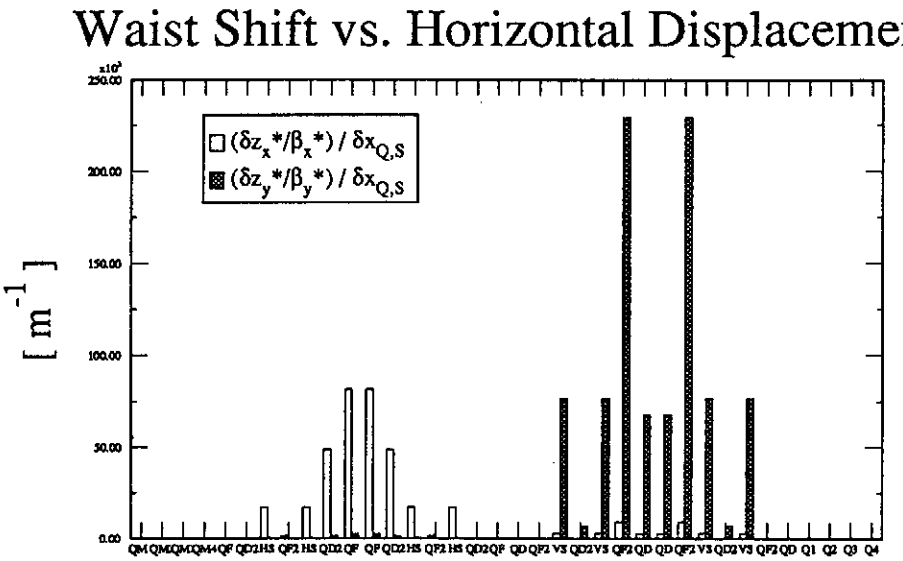

Figure 12: Ratio of IP waist-shift (normalized by the beta-function) to quadrupole and sextupole horizontal displacement.

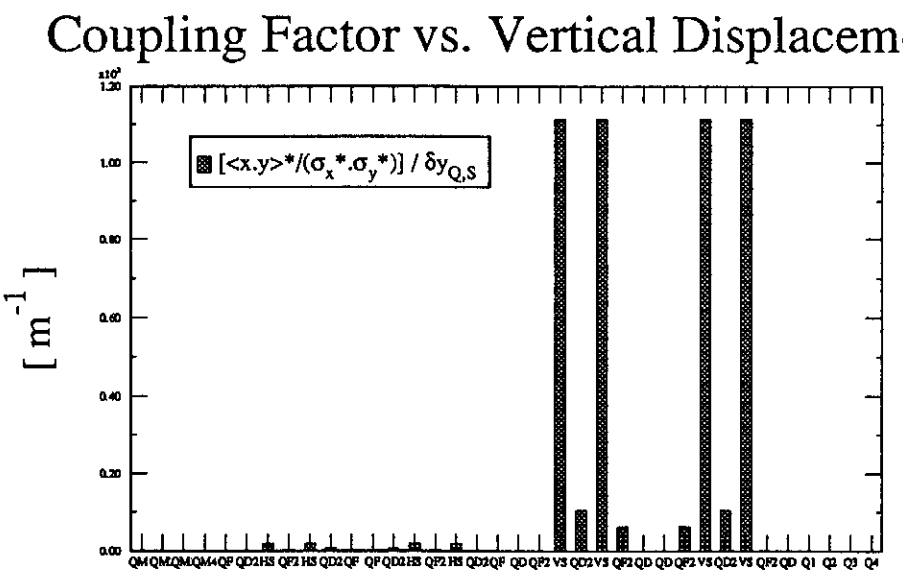

Figure 13: Ratio of IP coupling to quadrupole and sextupole vertical displacement.

The luminosity loss for fixed transverse displacements of each quadrupole and sextupole is plotted in Fig.14. In this calculation, one beam is assumed perfect while the other one is affected by the combined effect of the position and angular offset of the central trajectory and of the dispersion due to the displacement errors. The effect of the waist shifts and *xy*-coupling on the luminosity will be included in a later version of FFADA. The luminosity loss is calculated from the second derivatives of the luminosity derived in DIFFLUM. The same effect is represented differently in Fig.15 by plotting the transverse displacement of each element inducing a 2% loss in luminosity. Since beam offsets at the IP will be corrected more rapidly than the dispersion-induced spot size growth, it is interesting to calculate the

loss of luminosity by assuming zero beam offset at the IP. Fig.16 plots the tolerance to transverse magnet displacements derived from 2% luminosity loss with beam offset set to zero. The loss of luminosity, mainly due to the dispersion, is calculated for a beam with 0.1% energy spread.

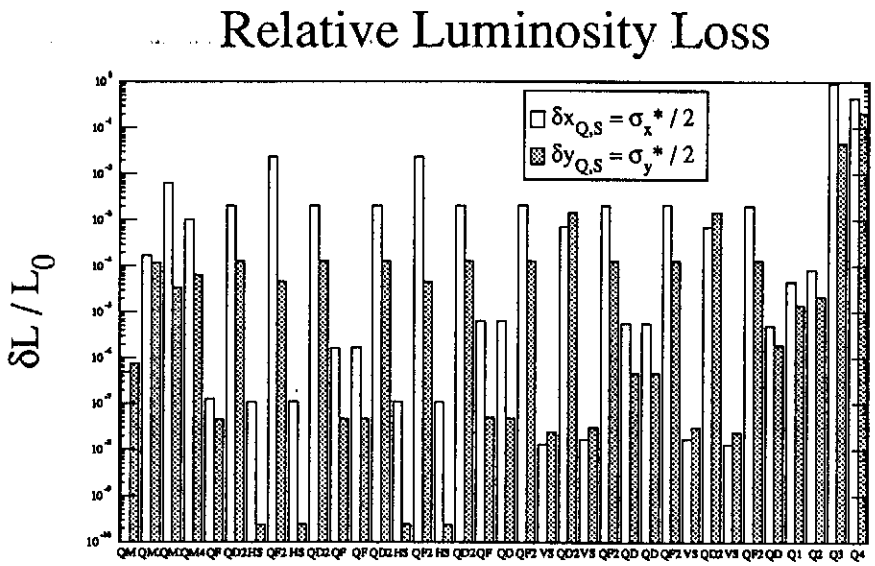

Figure 14: Relative luminosity loss for fixed quadrupole and sextupole transverse displacement.

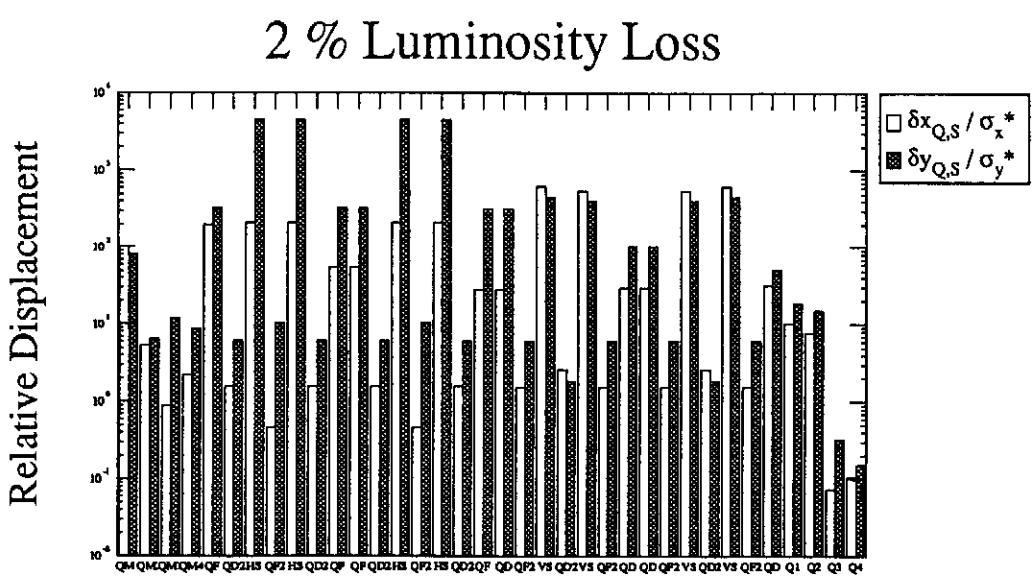

Figure 15: Quadrupole and sextupole transverse displacement for 2% luminosity loss.

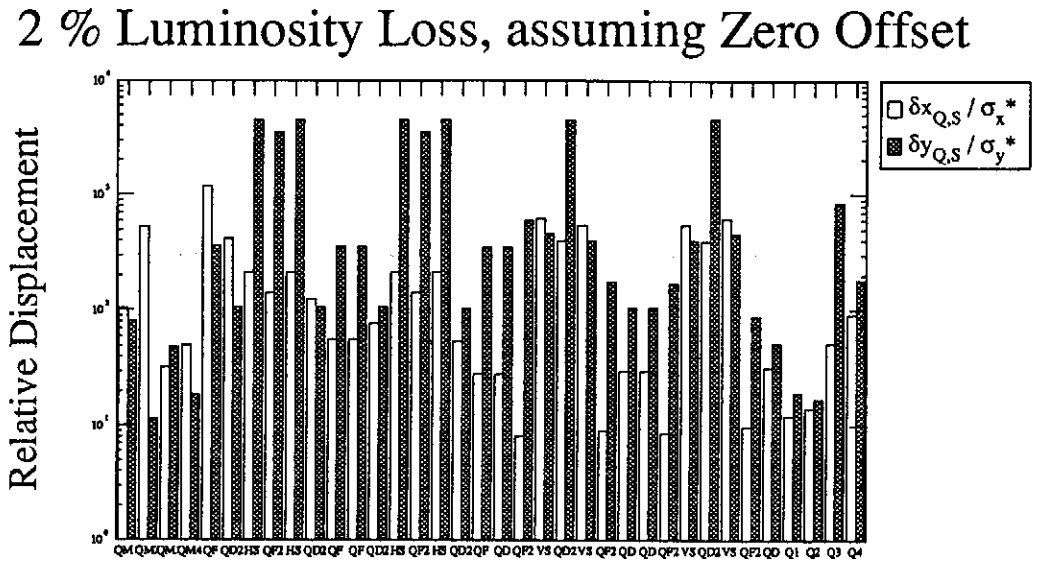

Figure 16: Quadrupole and sextupole transverse displacement for 2% luminosity loss assuming zero beam offset at the IP.

6.2.2 Transverse rotations

By transverse rotations, we mean rotations around the y-axis in the horizontal plane, or rotations around the x-axis in the vertical plane. We have adopted MAD [6] conventions which assume that the rotation axis is located at the entrance of the rotated magnet. The effect of transverse rotation errors is exactly parallel to the one of transverse displacements. Figs.17–20 show the dependence at the IP of the position of the central trajectory, the dispersion, the position of the waist and the xy-coupling on the angles $\delta x'$ and $\delta y'$ of horizontal and vertical rotations of each magnets.

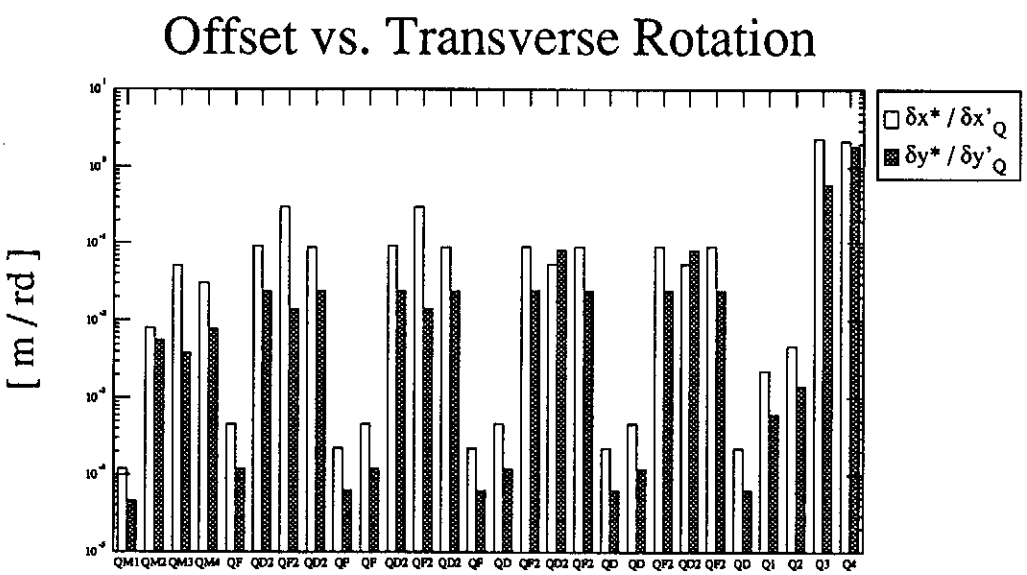

Figure 17: Ratio of IP offset to angle of quadrupole rotation in the horizontal and vertical plane.

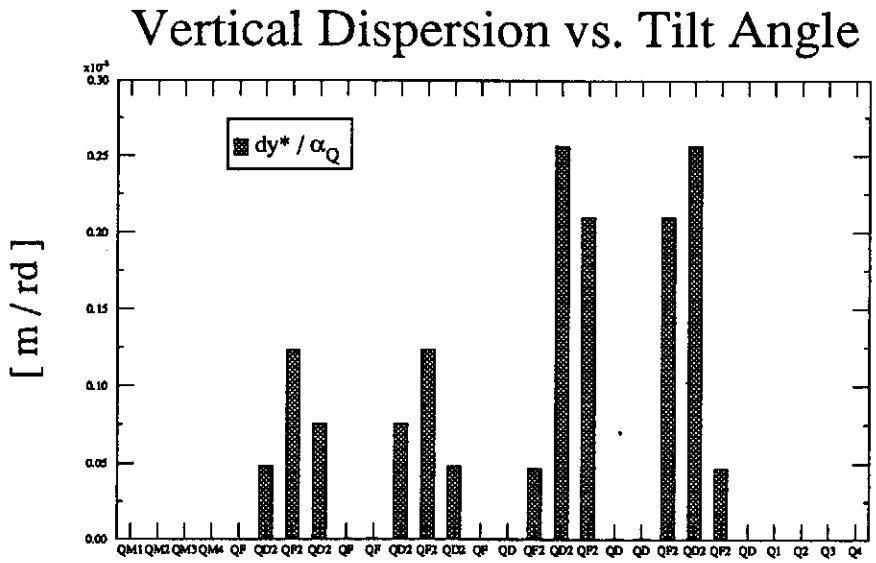

Figure 18: Ratio of IP dispersion to angle of quadrupole and sextupole rotation in the horizontal and vertical plane.

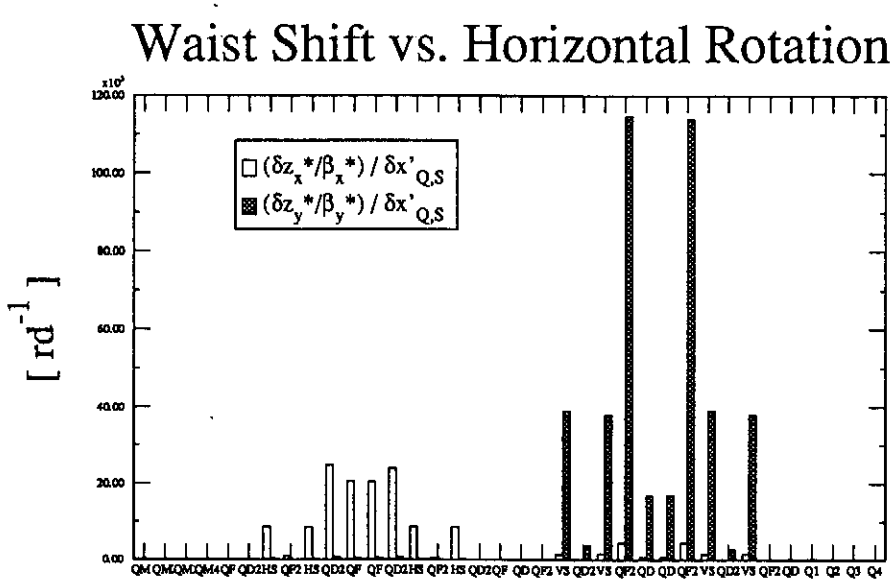

Figure 19: Ratio of IP waist shift (normalized by the beta-function) to angle of quadrupole and sextupole rotation in the horizontal plane.

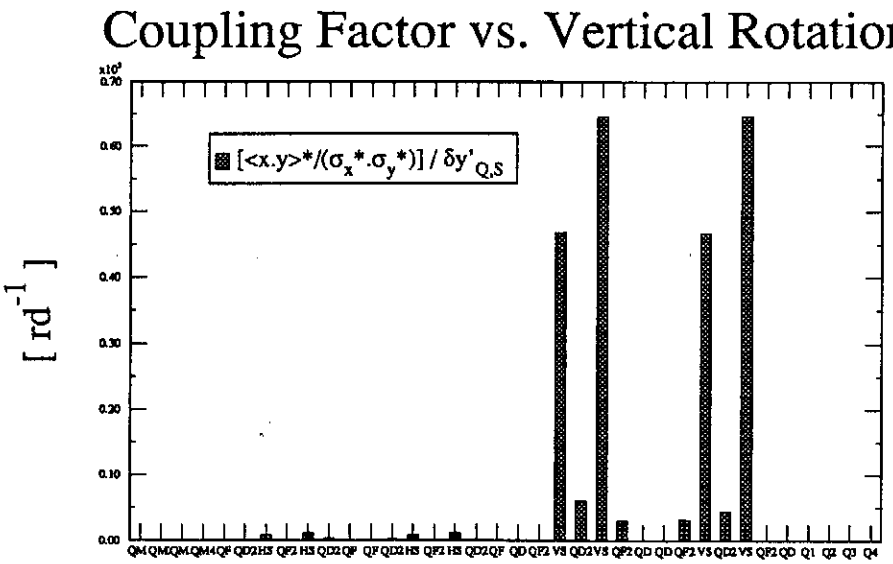

Figure 20: Ratio of IP coupling to angle of quadrupole and sextupole rotation in the vertical plane.

6.2.3 Longitudinal displacement

A longitudinal displacement of a **quadrupole** creates :

- at 1st order:
  - a horizontal position and angular dispersion at the IP if the dispersion at the quadrupole location is non zero (see Fig.21) ;
  - a normal gradient error which in turn produces a longitudinal shift δz^* of the horizontal and vertical β–waist at the IP (see Fig.22).

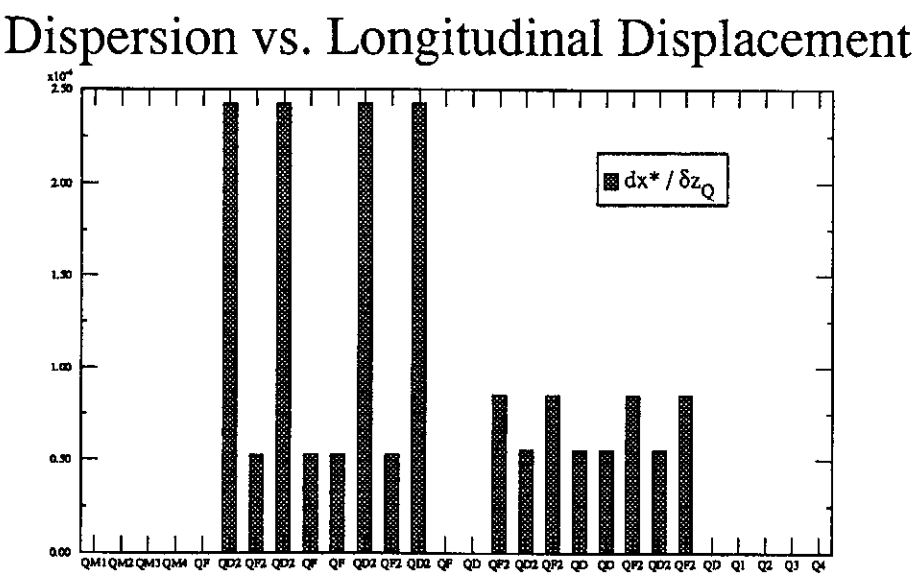

Figure 21: Ratio of IP horizontal dispersion to quadrupole longitudinal displacement.

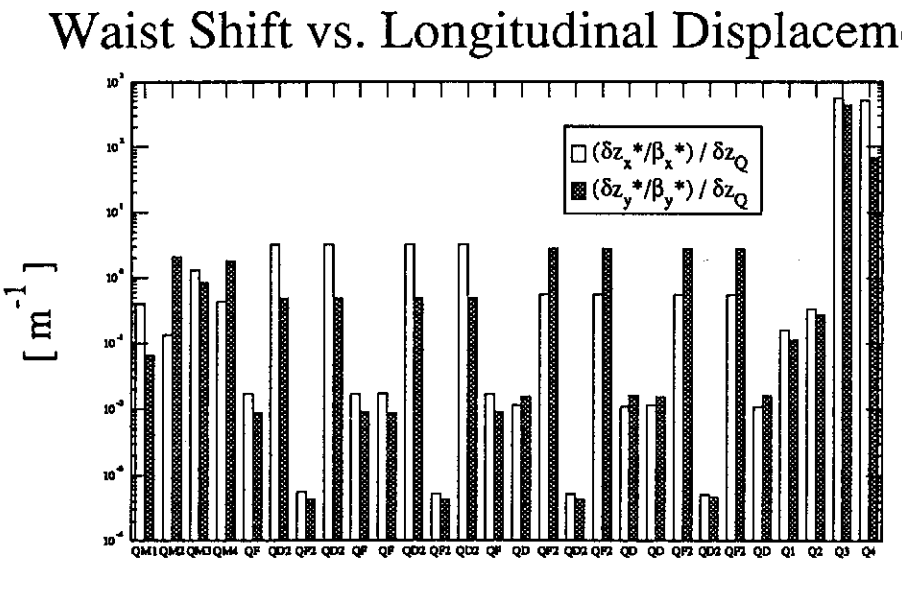

Figure 22: Ratio of IP waist shift (normalized by the beta function) to quadrupole longitudinal displacement.

6.2.4 Tilt rotation

By tilt (or skew) rotation we mean rotation of a magnet around the *z*-axis at its centre. Such a rotation of a **quadrupole** creates :

- at 1st order:
  - a vertical dispersion at the IP (see Fig.23) ;
  - *xy*-coupling at the IP (see Fig.24).

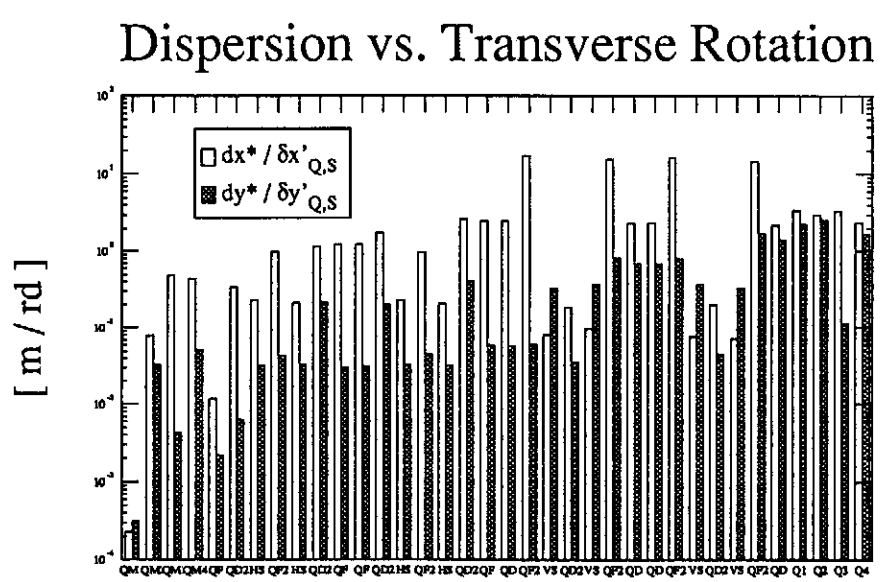

Figure 23: Ratio of IP vertical dispersion to quadrupole tilt angle (z-axis).

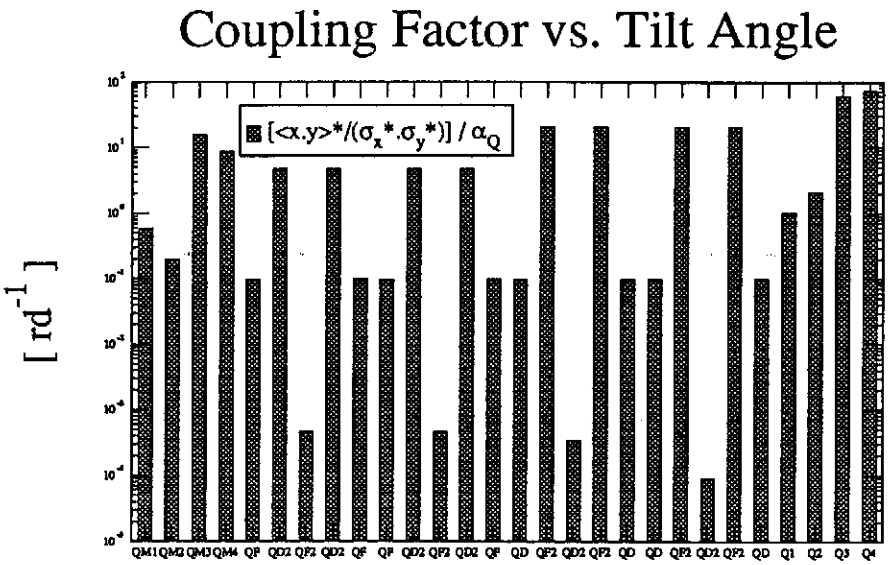

Figure 24: Ratio of IP coupling to quadrupole tilt angle (z-axis).

6.2.5 Gradient error

A quadrupole gradient error, exactly like a quadrupole longitudinal displacement, generates horizontal position and angular dispersion (see Fig.25), horizontal and vertical β-waist shifts (see Fig.26) at the IP.

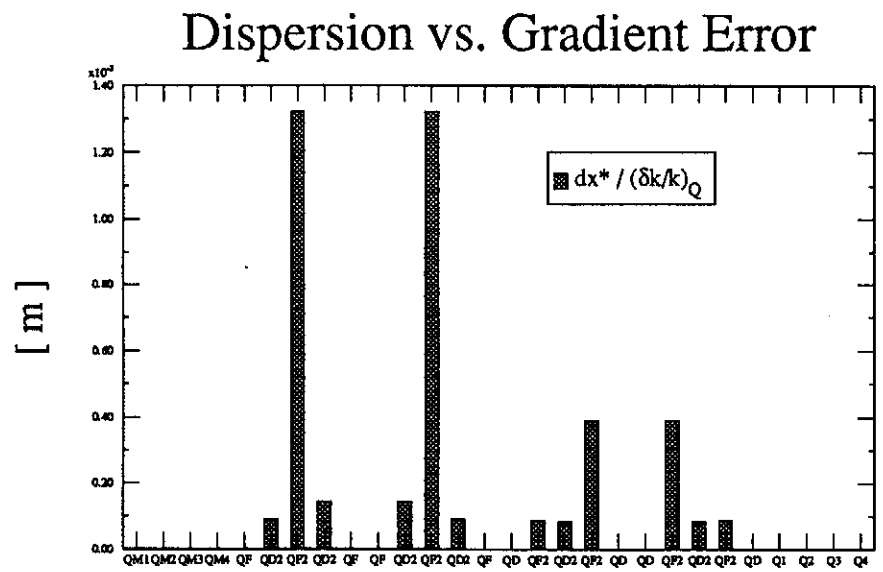

Figure 25: Ratio of IP horizontal dispersion to quadrupole relative gradient error.

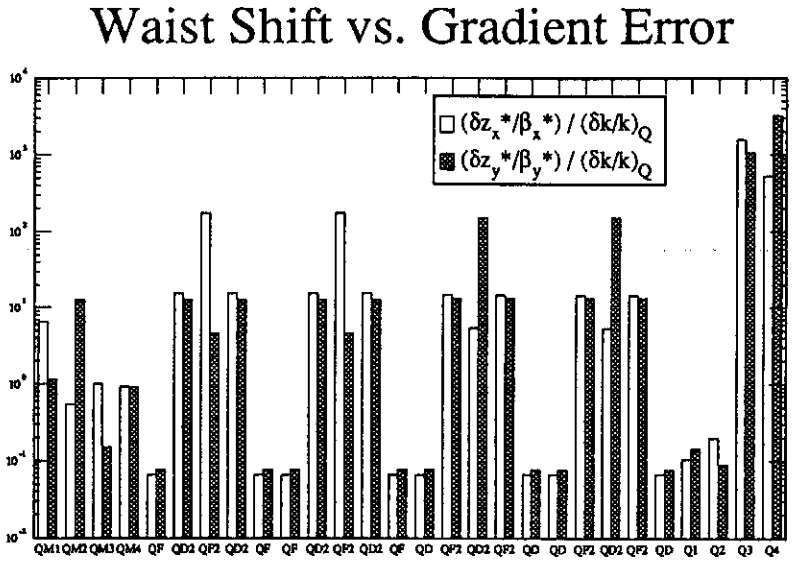

Figure 26: Ratio of IP waist shift (normalized to the beta function) to quadrupole relative gradient error.

6.2.6 Tolerances on transverse displacements

Finally, tolerances on the amplitude of the transverse motion of the magnets can be derived from the analysis of the loss of luminosity induced by these motions. One considers, on one hand, the effect of uncorrelated motion with the same rms amplitude of all the magnets of the electron and positron FFS, except the last doublet quadrupoles, and on the other hand the displacement of the 4 quadrupoles of the two opposing doublets. The results of this analysis are written in the second output file from the ERROR module, reproduced in Appendix E. We discuss below the main results.

If the relative beam offset at the IP is not corrected (like for fast vibrations for instance), the loss of luminosity is dominated by this offset. Assuming uncorrelated transverse motion of all the magnets (except the last doublets) of rms amplitude $\sigma_{x,\mathrm{QS}}$ and $\sigma_{y,\mathrm{QS}}$, the average horizontal and vertical beam relative offsets at the IP are given by

$$\begin{aligned} \overline{\delta x} &= 1.52\ \sigma_{x,\mathrm{QS}} \\ \overline{\delta y} &= 0.39\ \sigma_{y,\mathrm{QS}} \end{aligned} \tag{3}$$

leading to the following loss of luminosity, at the lowest order

$$\overline{\delta\mathcal{L}/\mathcal{L}_0} \;=\; -\Big\{0.58\,\big(\sigma_{x,\mathrm{QS}}/\sigma_x^*\big)^2 + 3.6\times 10^{-2}\big(\sigma_{y,\mathrm{QS}}/\sigma_y^*\big)^2\Big\}\,. \tag{4}$$

The fact that the horizontal beta-function is much larger than the vertical one along the FFS (see Fig.1) explains why the vertical coefficient is smaller than the horizontal one in the above equations.

If the offset is corrected by beam steering (for sufficiently slow vibrations), the loss of luminosity is then dominated by the spot size growth induced by the horizontal and vertical dispersions at the IP. The average dispersions are given by

$$\begin{aligned} \overline{d_x^*} &= 74.8\ \sigma_{x,\mathrm{QS}} \\ \overline{d_y^*} &= 24.3\ \sigma_{y,\mathrm{QS}} \end{aligned} \tag{5}$$

leading to the following luminosity loss

$$\overline{\delta\mathcal{L}/\mathcal{L}_0} = -\left\{ 4.3 \times 10^{-3} \left(\sigma_{x,\mathrm{QS}}/\sigma_x^*\right)^2 + 2.75 \times 10^{-4} \left(\sigma_{y,\mathrm{QS}}/\sigma_y^*\right)^2 \right\} . \tag{6}$$

for bunches with 0.1% rms relative energy spread.

As for the quadrupoles (Q3,Q4) of the last doublets, the loss of luminosity, without beam steering, is governed mainly by the relative displacements δx_{Q3} and δy_{Q3} of the opposing focusing Q3 quadrupoles, and $\delta x_{\mathrm{Q4}}$and δy_{Q4} of the opposing de-focusing Q4 quadrupoles, (see Appendix A). At leading order the luminosity loss is given by

$$\delta\mathcal{L}/\mathcal{L}_0 = -\left[\left(1.91 \frac{\delta x_{\mathrm{Q3}}}{\sigma_x^*} - 1.33 \frac{\delta x_{\mathrm{Q4}}}{\sigma_x^*} \right)^2 + \left(0.43 \frac{\delta y_{\mathrm{Q3}}}{\sigma_y^*} - 0.92 \frac{\delta y_{\mathrm{Q4}}}{\sigma_y^*} \right)^2 \right] \tag{7}$$

With steering correction, the system is also sensitive to the coherent motion of the opposing quadrupoles, i.e. to the sum of their displacements Σx_{Q3}, Σy_{Q3}, $\Sigma x_{\mathrm{Q4}}$and Σy_{Q4}. The loss of luminosity is given by

$$\begin{aligned}
\delta\mathcal{L}/\mathcal{L}_0 = & -\left(3.4 \times 10^{-7} \left(\frac{\delta x_{\mathrm{Q3}}}{\sigma_x^*}\right)^2 + 2.1 \times 10^{-8} \left(\frac{\delta x_{\mathrm{Q4}}}{\sigma_x^*}\right)^2 - 1.7 \times 10^{-7} \left(\frac{\delta x_{\mathrm{Q3}} \delta x_{\mathrm{Q4}}}{\sigma_x^{*2}}\right) \right) \\
& -\left(1.8 \times 10^{-7} \left(\frac{\delta y_{\mathrm{Q3}}}{\sigma_y^*}\right)^2 + 1.3 \times 10^{-8} \left(\frac{\delta y_{\mathrm{Q4}}}{\sigma_y^*}\right)^2 - 9.5 \times 10^{-8} \left(\frac{\delta y_{\mathrm{Q3}} \delta y_{\mathrm{Q4}}}{\sigma_y^{*2}}\right) \right) \\
& +\left(3.5 \times 10^{-6} \left(\frac{\Sigma x_{\mathrm{Q3}}}{\sigma_x^*}\right)^2 + 1.1 \times 10^{-6} \left(\frac{\Sigma x_{\mathrm{Q4}}}{\sigma_x^*}\right)^2 - 3.9 \times 10^{-6} \left(\frac{\Sigma x_{\mathrm{Q3}} \Sigma x_{\mathrm{Q4}}}{\sigma_x^{*2}}\right) \right) \\
& +\left(1.4 \times 10^{-8} \left(\frac{\Sigma y_{\mathrm{Q3}}}{\sigma_y^*}\right)^2 + 3.1 \times 10^{-7} \left(\frac{\Sigma y_{\mathrm{Q4}}}{\sigma_y^*}\right)^2 + 1.3 \times 10^{-7} \left(\frac{\Sigma y_{\mathrm{Q3}} \Sigma y_{\mathrm{Q4}}}{\sigma_y^{*2}}\right) \right)
\end{aligned} \tag{8}$$

with 0.1% rms relative energy spread.

6.3 Effect of Ground Motion

The effect of ground motion can be estimated from the integrated spectrum of vibrations $\sigma_{\mathrm{V}}(f_0)$ which gives the rms amplitude of vibrations integrated above the frequency f_0. The three spectra plotted in Fig.27 correspond to measurements of vertical vibrations at three different sites: two at CERN (LEP and TT2A tunnels) and one at Protvino (UNK tunnel). Taking the LEP or UNK spectra as a reference, we can estimate the characteristic frequency corresponding to a 2% loss of luminosity loss from the 3 following sources:

1. ***motion of the most sensitive of all magnets, except the last doublet quadrupoles.*** As shown in Figs.14 or 15, these are the two de-focusing quadrupoles QD2 located next to the vertically correcting sextupoles VS. 2% luminosity is lost if one of them is displaced by 120 nm corresponding to about 0.2 Hz frequency.
2. ***uncorrelated motion of all the magnets, except the last doublet quadrupoles.*** Equation 4 gives the rms amplitude of 50 nm corresponding to a frequency of about 0.3 Hz.
3. ***motion ,of the most sensitive of all quadrupoles,*** namely the last (de-focusing) quadrupole Q4 of the last doublet. Equation 7 leads to a relative displacement of the 2 opposing Q4 magnets of 10 nm corresponding to the frequency of about 0.8 Hz.

Assuming that one can measure the effect of such displacements on the beams and correct it, the above characteristic frequencies indicate that the foreseen 10 Hz repetition frequency should be fast enough to feed the correction system.

This analysis can be repeated in the case where beams are steered into collision. The luminosity loss is then due to dispersion at the IP. As shown in Fig.16 and in Eqs.6 and 8, the tolerances are much bigger but the correction system will be more involved and hence much slower.

In this analysis we have neglected the effect of spatial correlations which must be studied more carefully. Also, vibrations can have other sources than ground motion. In particular it would be important to know the vibration spectrum of the superconducting quadrupoles in their cryostat.

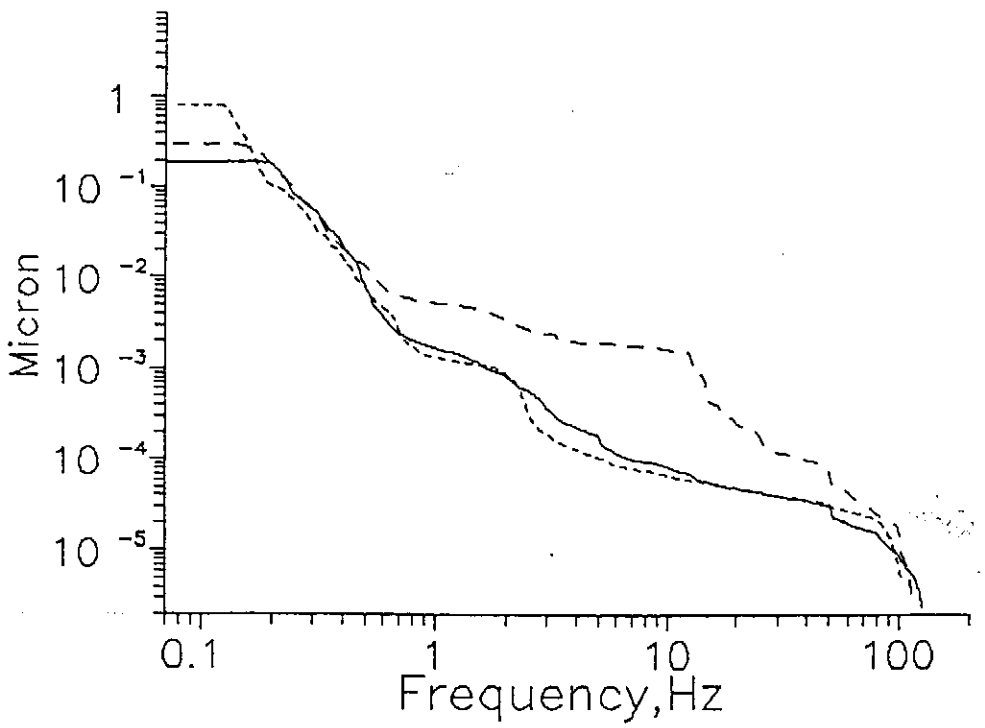

Figure 27: Integrated Spectrum of vibrations in the TT2A tunnel measured VLEPP probes (vertical vibrations), from Ref.[3].

7 The Last Doublet Superconducting Quadrupoles

The required characteristics of the quadrupoles, namely a gradient of 250 T/m and an aperture of a few centimeters, and the possibility to use superfluid helium lead to consider the existing design of the LHC lattice quadrupole [4] as the basic concept. Moreover, two prototypes of these quadrupoles have been tested and achieved their design gradient [10]

7.1 The magnet design

A cross section of the proposed magnet in its cryostat is shown in Fig.28 and its main parameters are given in Table 1.

General Parameters	
Gradient	250 T/m
Physical aperutre	48 mm
Magnetic length	1.920 m and 1.274 m
Overall current density	560 A/mm^2
Peak field in conductor (Quad only)	7.8 T
Peak field in conductor (Quad + 3T-Solenoid)	8.4 T
Critical field at 1.8 K	9.3 T
Current	15,900 A
Radial Dimensions	
Inner coil diameter	56 mm
Outer coil diameter	108 mm
Helium vessel inner diameter	172 mm
Helium vessel outer diameter	192 mm
Mean diameter of 4.2K screen	272 mm
Mean diameter of 70K screen	352 mm
Vacuum tank inner diameter	432 mm
Vacuum tank outer diameter	442 mm
Weight per unit length	305 Kg/m

Table 1 Magnet parameters

Since the quadrupoles are placed inside of the detector solenoid whose 3 Tesla magnetic field would saturate iron, the iron core foreseen for the LHC magnet must be removed. The 5% reduction in gradient can be compensated by increasing the current in the same proportion up to 15900 A. Even without iron core, the stray-field of the quadrupole, in the radial direction, decreases fast enough to not perturb the physics (see Fig.29). For example, it is 5×10^{-3} Tesla at 60 cm radius.

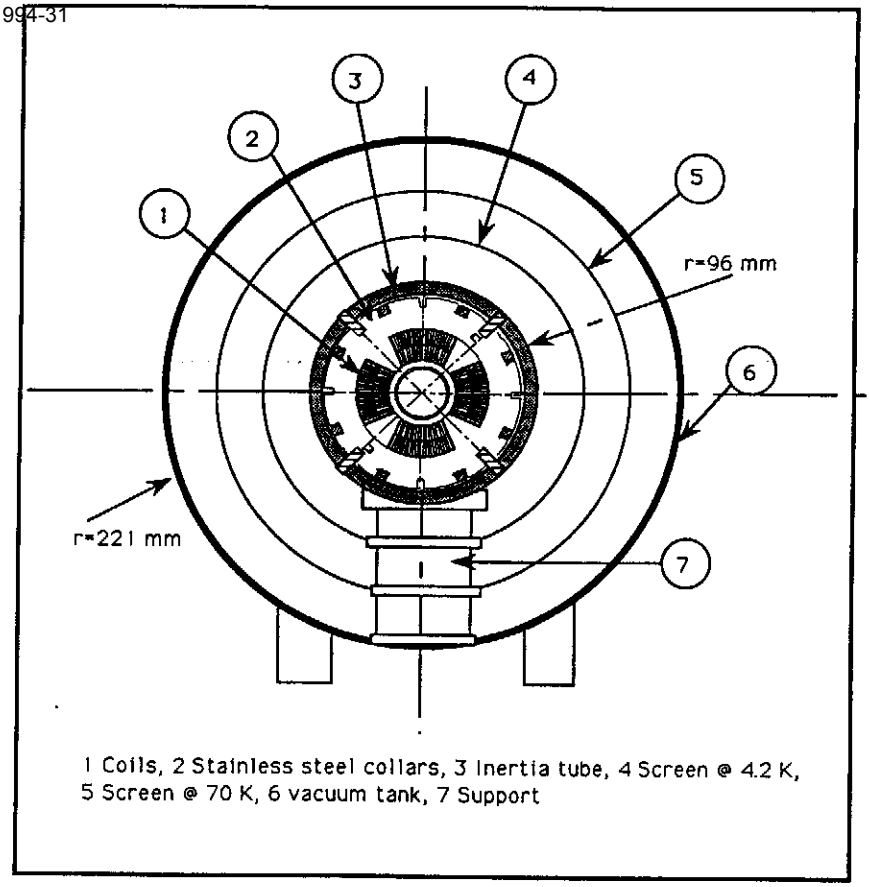

Figure 28: Cross-section of the last doublet superconducting quadrupoles.

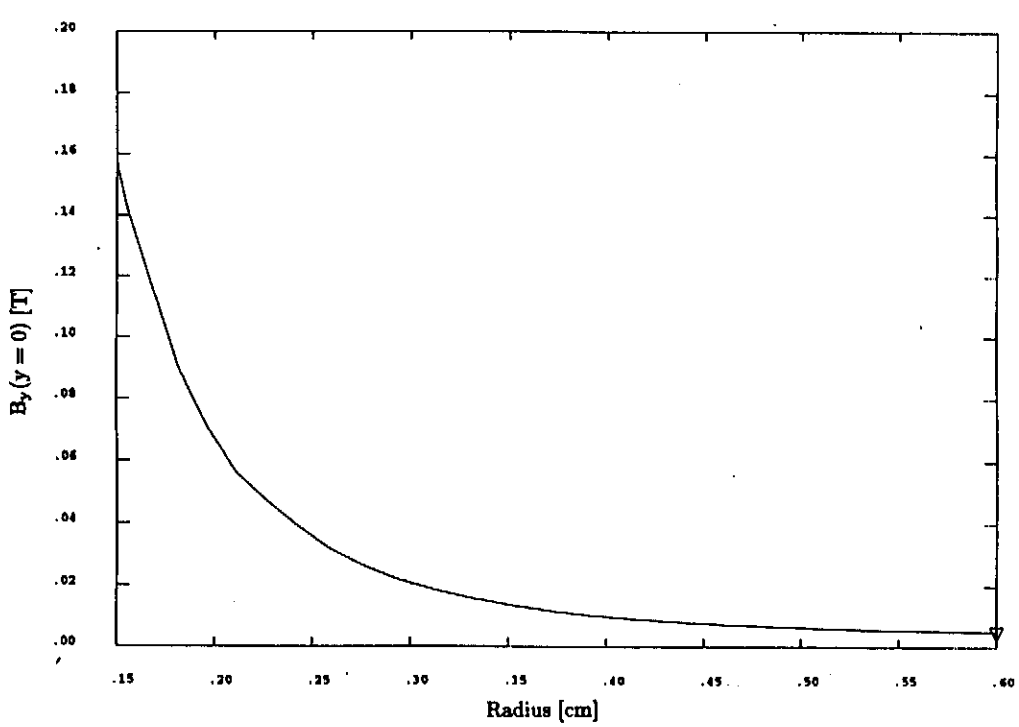

Figure 29: Transverse stray magnetic field B_y(y=0) of the superconducting quadrupoles.

7.2 Description

The conductor is a keystone cable whose bare dimensions are approximately 13.05 x (1.7-:-2.16). It should be specified to withstand a 3 Tesla parallel magnetic field in addition to the quadrupole self field. As for the LHC lattice quadrupoles, the coils are made of two shells without splice between them. The stainless steel collars are strong enough to cancel the electromagnetic forces. The collaring process consist of setting subsequent pairs of collars in direction perpendicular to each other along the entire coil length. The prestress, needed to avoid any motion in the coils during excitation, is given by the insertion of eight tapered keys at the outside of the collars. As previously explained, there is no iron core surrounding the magnet. The collared coil is then centred in the helium vessel by mean of four keys. The mechanic centre of the coil is defined by the intersection of the two perpendicular planes of two opposite keys. The helium vessel is a rough tube, machined precisely (± 25 μm) to give the correct position of the centring keys. Its thickness is sufficient to withstand the pressure drop in case of quench and to give the axial rigidity necessary to reduce the magnet sag. Since the working temperature is 1.8 K, a 4.2 K screen is necessary ($(70^4 - 1.8^4)/(4.2^4 - 1.8^4) = 8 \times 10^5$). Another screen at a temperature of about 70 K intercepts the radiations coming from the room temperature vacuum tank. The distances between parts at different temperatures are, in a first approach, chosen to be 40 mm.

7.3 Alternative

Using Nb_3Sn instead of NbTi as superconducting material would lead to one of the following changes:

1. use of 4.2 K helium instead of 1.8 K superfluid helium. This option would permit to remove one screen and to decrease the outer diameter by about 80 mm;
2. work at 1.8 K with the same gradient and increase the magnet aperture since the superconductor can stand at a higher magnetic field;
3. work at 1.8 K with the same aperture and increase the gradient.

Although these options are attractive, the Nb_3Sn technology is not yet well mastered: it would lead to challenging R&D work and to a modified design since the mechanics and the quench protection in particular would be more constraining.

7.4 Tolerances to higher multipoles

The field quality can be defined by the coefficients of multipolar expansion of the field:

$$B_y + iB_x = B(r_0) \sum_{n \geq 2} (b_n + ia_n)(z/r_0)^{n-1} \tag{9}$$

where r_0 is a reference radius and $z = (x + iy)$ is the complex transverse coordinate. The multipole coefficients leading to a 2% spot size growth (in the most sensitive plane and for the worst quadrupole) are given in Table 2 for r_0 = 1 cm. In practice, we believe that all the b_n and a_n coefficients can be made smaller than 7×10^{-4} at a 1 cm radius.

n	3	4	5	6	7
normal $b_n/10^{-3}$	1.8	22	230	1690	13,330
skew $a_n/10^{-3}$	0.67	7.5	69	590	3,770

Table 2 Required field quality multipole coefficients

7.5 Effect of the main solenoid

The detector solenoid is likely to extend over part or all of the two opposing doublets, precluding the use of iron in the magnets. Operating the iron-free quadrupole in a longitudinal solenoid field of 3 T shifts the magnetic field in the conductor from 7.8 T to 8.4 T, that is roughly 10% lower than the critical field of 9.3 T at the current density of 560 A/mm^2. If necessary, the safety margin can be increased either by relying on progress to come on the maximum current sustained in SC cables or by reducing the focusing gradient of about 10 %.

Optics-wise, the detector solenoid field is harmless as long as it is less than 6 m long and therefore does not extend, even partially, over the last doublet. On the contrary, if it superimposes over the quadrupole field it induces a blow up of the horizontal and vertical beam sizes up to 1.5 μm at the IP. However this effect can be compensated completely with two skew quadrupoles (one per beam) located at both ends of the solenoid.

8 Beam Separation after collision

Beam separation in TESLA can be done outside of the detector in the 74 m long drift space between the 2 doublets of the last telescope (see Fig.1). The separation scheme presented in [1] is based on a static system which superimposes an electrostatic and a magnetic field in such a way that the incoming trajectory is not bent in order to prevent synchrotron radiation from hitting the detector. Three constraints have to be fulfilled for the separation:

1. the beam-beam kick at the unwanted crossing (i.e.150 m from the IP) must be small compared to the intrinsic angular divergence $\sigma_{x'} \simeq \epsilon_x/\sigma_x$ of the incoming beam. This divergence is 5 μrd at the crossing point where it is maximum, and is larger than 0.45 μrd anywhere in the chromatic correction section. On the other hand, the beam-beam deflection angle is given by $\Delta x' = 2r_e N/\gamma\Delta x$ where r_e is the classical electron radius, N the bunch population, γ the Lorentz factor and Δx the beam separation. With the TESLA parameters the condition for a negligible beam-beam kick is $\Delta x \gg 0.12$ mm. Notice that this condition might not be necessary if the outgoing beam is already in a different beam line before the unwanted crossing.
2. the outgoing beam must be sufficiently displaced from the axis at the end of the separator for a septum magnet to be installed. This septum magnet will further deviate[12] the spent beam to its dump or recycling system.
3. the deviation angle of the outgoing beam must be larger, with some margin, than the emission angle of the beamstrahlung photons, namely $\pm$0.5 mrd [13]. This is necessary in order to protect the edges of the septum magnets from the burst of beamstrahlung photons.

The electrostatic separators installed in LEP can be used to achieve the above requirements. They develop [6] a transverse electric field of 3 MV/m across a 10 cm gap and over a unit length of 4 m. To cancel the transverse force acting on the incoming beam, the needed magnetic field is 0.01 T. After 64 m (16 units), the deflection angle is 1.54 mrd and the outgoing beam is 4.9 cm off axis. The beam-beam kick is therefore clearly negligible while the installation of the septum magnets looks feasible. The tolerance and the field quality required for such system should however be carefully studied.

Separators with 6–8 MV/m gradient and 1–2 cm gap have been designed for LEAR at CERN. They rely on good vacuum conditions, no synchrotron radiation and loose sparking tolerances. These conditions may be difficult to meet in the TESLA interaction region.

Aknowledgements: We would like to thank S. Fartoukh and R. Brinkmann for pointing out a mistake in the calculation of the dipersion errors in the program FFADA. This mistake has been corrected in the present manuscript.

References

[1] O. Napoly, "A Large Aperture Final Focus System fro TESLA",Proc.of XIVth PAC, Washington DC, USA (1993).

[2] B. Dunham and O. Napoly, "FFADA, Final Focus Automatic Design and Analysis", Saclay Preprint DAPNIA/SEA 94–06 and Proc. of EPAC94 Conf., London, Great Britain, 1994.

[3] V.M. Juravlev, A.A. Sery, A.I. Sleptsov., W. Coosemans, G. Ramseier and I. Wilson ,"Investigations of Power and Spatial Correlation Characteristics of Seismic Vibrations in the CERN LEP Tunnel for Linear Collider Studies", CERN-SL/93–53.

[4] J.M. Baze et al., "Design and Fabrication of the Prototype Superconducting Quadrupole for the CERN LHC Project", MT12 Conf. Leningrad, Russia,1991
J.M. Rifflet et al., "Status of the Fabrication and test of the Prototype LHC Lattice Quadrupole Magnets", MT13 Conf. Victoria, Canada, 1991.

[5] B. Goddard, W. Kalbreier, Transactions on Electrical Insulation, **24**,4,444–453(1993).

[6] H. Grote and F.C. Iselin, "The MAD Program", CERN/SL/90–13 (AP) Rev.3 (Jan.1993).

[7] R.V. Servranckx, K.L. Brown, L. Schachinger and D. Douglas, "Users Guide to the Program DIMAD", SLAC Report 285 UC-28 (A) (May 1985).

[8] K. Hirata, K. Oide and B. Zotter, Phys. Letters B **224**, 437 (July 1989).

[9] O. Napoly, Part. Acc. **40/4**, 181 (1993)

[10]J.M. Rifflet et al., "Cryogenic and Mechanical Measurements of the first two LHC Lattice Quadrupoles Prototypes", EPAC94 Conf., London, Great Britain, 1994.

[11]A. Drozhdin, "Extraction of the Disrupted Beam into the Beam Capture Section", in preparation.

[12]D. Schulte, "Background in the Interaction Region of TESLA", in preparation.

List of Figures

Appendix A: Optics of the FFS beam line, in MAD format

```
TITLE &
" 4-lens telescopic (  68.1 x  98.6 )=(  8.5 x  3.3 )*(  8.0 x 30.0 ) FFS     "
!
! DATE AND TIME:     10/07/94  18.27.04
!
! FILE:              td400.mad
!
DM1: DRIFT, L=0.35
DM2: DRIFT, L=16.889658319403
DM3: DRIFT, L=4.859860861125
DM4: DRIFT, L=1.428784
DM5: DRIFT, L=0.7717838
QM1: QUADRUPOLE, L=0.3, K1=0.197233601043
QM2: QUADRUPOLE, L=0.3, K1=-0.693280695796
QM3: QUADRUPOLE, L=0.328160498306, K1=1.678838
QM4: QUADRUPOLE, L=0.546228892727, K1=-1.678838
BMH: SBEND, L=LB, ANGLE=0.6E-3
BMV: SBEND, L=LB, ANGLE=-0.6E-3
DR: DRIFT, L=LB
DR1: DRIFT, L=LD
DQ: DRIFT, L=LQ
QF: QUADRUPOLE, L=LQ, K1=0.087814944322
QD: QUADRUPOLE, L=LQ, K1=-0.087814946645
QF2: QUADRUPOLE, L=2.0*LQ, K1=0.087814916657
QD2: QUADRUPOLE, L=2.0*LQ, K1=-0.087814918572
HS: SEXTUPOLE, L=LS, K2=9.352714531523
VS: SEXTUPOLE, L=LS, K2=47.832909758188
D1: DRIFT, L=0.85
D2: DRIFT, L=0.940412927576
D3: DRIFT, L=74.074745300458
D4: DRIFT, L=0.35
D5: DRIFT, L=3.0
Q1: QUADRUPOLE, L=0.3, K1=0.386085187721
Q2: QUADRUPOLE, L=0.3, K1=-0.386118652087
Q3: QUADRUPOLE, L=1.274149373084, K1=0.2997925
Q4: QUADRUPOLE, L=1.920443722635, K1=-0.2997925
TELEM: LINE=(DM1,QM1,DM2,QM2,DM3,QM3,DM4,QM4,DM5)
DICELLH: LINE=(QF,BMH,QD2,DR1,HS,QF2,HS,DR1,QD2,BMH,QF)
DICELLH2: LINE=(QF,BMH,QD2,DR1,HS,QF2,HS,DR1,QD2,BMH,DQ)
DICELLV1: LINE=(DQ,BMV,QF2,DR1,VS,QD2,VS,DR1,QF2,BMV,QD)
DICELLV: LINE=(QD,BMV,QF2,DR1,VS,QD2,VS,DR1,QF2,BMV,QD)
CCSH: LINE=(DICELLH,DICELLH)
CCSV: LINE=(DICELLV,DICELLV)
CCS: LINE=(CCSH,CCSV)
DBLT: LINE=(Q3,D4,Q4)
TELE: LINE=(D1,Q1,D2,Q2,D3,DBLT,D5)
FFS: LINE=(TELEM,CCS,TELE)
LFOD := 16.44192
LQ := 0.5
LS := 1.0
LB := LFOD-2.0*LQ
LD := LB-LS
!  Beta at the Entrance of the FFS
INIT0: BETA0, &
     , BETX=   113.445 ,BETY=    19.482
RETURN
```

Appendix B: Output from DBLT Module

```
   ************************************************************************
   *                                                                      *
   *                                DBLT                                  *
   *                                                                      *
   *                    DATE:10/07/94   TIME:18:33:03                     *
   *                                                                      *
   ************************************************************************
*****************************************************************************
*                                                                           *
*                          BASIC INPUT PARAMETERS                           *
*                                                                           *
*****************************************************************************

  Energy/beam                          [GeV]  :          250.000
  Horizontal beta*_x                    [mm]  :           24.462
  Vertical   beta*_y                    [mm]  :            2.004
  Horizontal normalized emittance        [m]  :        2.000E-05
  Vertical   normalized emittance        [m]  :        1.000E-06
  Bunch length                          [mm]  :        1.000E+00
  Bunch population                            :        5.000E+10
  Repetition rate                       [Hz]  :        8.000E+03

 Last drift
  Length                                 [m]  :            3.000

 Last quadrupole
  Length                                 [m]  :            1.920
  K1                                   [m-2]  :           -0.300
  Aperture diameter                     [mm]  :           48.000

 Last before one drift
  Length                                 [m]  :            0.350

 Last before one quadrupole
  Length                                 [m]  :            1.274
  K1                                   [m-2]  :            0.300
  Aperture diameter                     [mm]  :           48.000

 Microvertex Detector
  Aperture diameter                     [mm]  :           30.000
*****************************************************************************
*                                                                           *
*                      MAXIMUM EXTENSION OF THE BEAM                        *
*                                                                           *
*****************************************************************************
 Total length       = 6.54E+00 m

 Maximum of beta_x  = 4.72E+03 m, at s =  6.481 m
  sigma_x           =  439.124 mu-m
 Aperture/sigma_x   =   54.654

 Maximum of beta_y  = 6.15E+03 m, at s =  3.960 m
  sigma_y           =  112.146 mu-m
 Aperture/sigma_y   =  214.006

 Clearance angle    = 3.67E+00 mrd
```

```
*****************************************************************************
*                                                                           *
*                          COLLIMATION REQUIREMENTS                         *
*                                                                           *
*****************************************************************************
 EMITTED PHOTONS AT THE VERTEX DETECTOR:

 Maximum of sigma_x =   476.79 mu-m, for 1-sigma emission at s =  6.545 m
 Maximum of sigma_y =   244.30 mu-m, for 1-sigma emission at s =  4.920 m

 Rectangular collimation at n_x * n_y sigma in Circular aperture :

       1/2 ( n_x /22.246 )**2 + 1/2 ( n_y /43.416 )**2 = 1

 EMITTED PHOTONS AT THE EXIT FACE OF THE OPPOSING DOUBLET:

 Maximum of sigma_x =  1429.03 mu-m, for 1-sigma emission at s =  5.270 m
 Maximum of sigma_y =   438.65 mu-m, for 1-sigma emission at s =  4.920 m

 Rectangular collimation at n_x * n_y sigma in Circular aperture :

       1/2 ( n_x /11.876 )**2 + 1/2 ( n_y /38.689 )**2 = 1

*****************************************************************************
*                                                                           *
*                                OIDE EFFECT                                *
*                                                                           *
*****************************************************************************
 l*_eff =  8.396E+00 m,  for the horizontal effect
 F1 horizontal =  1.062E+02
 F2 horizontal =  4.598E+03
 F1 vertical   =  6.295E+00
 F2 vertical   =  2.731E+01

 Horizontal Oide limit:  sigx =  4.115E+02 nm
 Vertical   Oide limit:  sigy =  2.251E+01 nm
*****************************************************************************
*                                                                           *
*                SYNCHROTRON RADIATION FROM LAST CCS BEND                   *
*                                                                           *
*****************************************************************************
 Bending radius                              [m] :  2.574E+04
 Bending field                               [T] :  3.240E-02

 Electron relative average energy loss       [%] :  5.129E-04
 Electron relative rms energy spread         [%] :  6.048E-04

 Photon critical energy                    [keV] :  1.347E+03
 Number of emitted photon per electron           :  3.092E+00
 Total number of emitted photon                  :  1.546E+11

 Emitted power per bend                      [W] :  8.217E+01
 Transv. deposition length (@ dblt entr.)  [m] :  5.081E-02
 Transv. deposition length (@ dblt exit )  [m] :  5.867E-02

*****************************************************************************
*                                                                           *
*                           END OF PROGRAM DBLT                             *
*                                                                           *
*****************************************************************************
```

Appendix C: Output from DIFFLUM Module

```
   ************************************************************************
   *                                                                      *
   *                              DIFFLUM                                 *
   *                                                                      *
   *                     DATE:16/12/94   TIME:18:15:19                    *
   *                                                                      *
   ************************************************************************

*****************************************************************************
*                                                                           *
*                            BEAM PARAMETERS                                *
*                                                                           *
*****************************************************************************

 Energy                            [GeV]     :         250.000
 Horizontal RMS at the IP          [nm]      :        1000.000
 Vertical   RMS at the IP          [nm]      :          64.000
 Horizontal angular divergence     [mu-rad]  :          40.880
 Vertical   angular divergence     [mu-rad]  :          31.937
 Longitudinal RMS                  [mm]      :           1.000
 Relative energy RMS                         :       1.000E-03
 NO WAKE
 Bunch population                            :       5.000E+10
 Repetition rate                   [Hz]      :       8.000E+03


*****************************************************************************
*                                                                           *
*                              - LUMINOSITY                                 *
*                                                                           *
*****************************************************************************


 Gaussian luminosity     [s-1.cm-2]  :  2.487E+33
 Hour-glass reduction factor         :       .949
 Nominal luminosity      [s-1.cm-2]  :  2.361E+33

 Horizontal disruption               :       .541
 Vertical   disruption               :      8.458
 Estimated pinch factor              :      2.260
 Luminosity with pinch   [s-1.cm-2]  :  5.336E+33

 Upsilon parameter                   :       .028
 Average relative energy loss  [%]   :      3.019
```

```
*****************************************************************************
*                                                                           *
*                    SECOND DERIVATIVES OF THE LUMINOSITY                   *
*                                                                           *
*****************************************************************************


 dL/Lo = - {  .250 * [(dx1-dx2)/sigx]**2
           +  .228 * [(dy1-dy2)/sigy]**2

           +  .114 * [(dxp1+dxp2)*sigz/sigx]**2
           +  .088 * [(dyp1+dyp2)*sigz/sigy]**2'

           + 1.25E-07 * [(dispx1+dispx2)/sigx]**2
           + 1.14E-07 * [(dispy1+dispy2)/sigy]**2

           + 1.25E-07 * [(dispx1-dispx2)/sigx]**2
           + 1.14E-07 * [(dispy1-dispy2)/sigy]**2

           + 5.68E-08 * [(dispxp1+dispxp2)*sigz/sigx]**2
           + 4.39E-08 * [(dispyp1+dispyp2)*sigz/sigy]**2

           + 5.68E-08 * [(dispxp1-dispxp2)*sigz/sigx]**2
           + 4.39E-08 * [(dispyp1-dispyp2)*sigz/sigy]**2 }


*****************************************************************************
*                                                                           *
*                              END OF DIFFLUM                               *
*                                                                           *
*****************************************************************************
```

Appendix D: Output from ERROR/QS_ERROR Module

```
**************************************************************************
*                                                                        *
*                              QS_ERROR                                  *
*                                                                        *
*                    DATE:10/07/94   TIME:18:33:14                       *
*                                                                        *
**************************************************************************

NUMBER OF DRIFTS                =   18

NUMBER OF DIPOLES               =   8

NUMBER OF QUADRUPOLES           =   28

NUMBER OF SEXTUPOLES            =   8

NUMBER OF MAGNETS OF THE LINE   =   44


TRANSFER MAP OF THE LINE (TRANSPORT)

       1.4685E-02   -5.4794E-03    0.0000E+00    0.0000E+00    3.4925E-12
      -3.6721E-06    6.8098E+01    0.0000E+00    0.0000E+00   -5.0321E-08
       0.0000E+00    0.0000E+00    1.0142E-02    4.6304E-04    0.0000E+00
       0.0000E+00    0.0000E+00    1.2060E-04    9.8601E+01    0.0000E+00

COMPARISON WITH INPUT TRANSFER MAP

       1.4684E-02    0.0000E+00    0.0000E+00    0.0000E+00    0.0000E+00
       0.0000E+00    6.8100E+01    0.0000E+00    0.0000E+00    0.0000E+00
       0.0000E+00    0.0000E+00    1.0142E-02    0.0000E+00    0.0000E+00
       0.0000E+00    0.0000E+00    0.0000E+00    9.8600E+01    0.0000E+00

     precision test =   1.6313E-05


**************************************************************************
*                                                                        *
*                        END OF PROGRAM QS_ERROR                         *
*                                                                        *
**************************************************************************
```

Appendix E: Output from ERROR/LUM_LOSS Module

```
   ************************************************************************
   *                                                                      *
   *                              LUM_LOSS                                *
   *                                                                      *
   *                     DATE:16/12/94   TIME:18:15:22                    *
   *                                                                      *
   ************************************************************************

*****************************************************************************
*                                                                           *
*                     QUADRATIC AVERAGES OVER 34 MAGNETS                    *
*                                                                           *
*****************************************************************************

   Relative beam offset    (without the last doublet) :

     SQRT<(dx1*-dx2*)**2>/sigx_QS =   1.5160E+00
     SQRT<(dy1*-dy2*)**2>/sigy_QS =   3.8981E-01

   Single beam dispersion  (without the last doublet) :

     SQRT<Dx1**2>/sigx_QS = SQRT<Dx2**2>/sigx_QS =   7.4840E+01
     SQRT<Dy1**2>/sigy_QS = SQRT<Dy2**2>/sigy_QS =   2.4334E+01


*****************************************************************************
*                                                                           *
*                 RELATIVE LUMINOSITY LOSS : NO CORRECTION                  *
*                                                                           *
*****************************************************************************

   Random & uncorrelated quad motion (without last doublet)

   dL/Lo = - { 5.77E-01 * (sigx_QS/sigx*)**2
             + 3.54E-02 * (sigy_QS/sigy*)**2 }

   Fixed motion of the last doublet :

   dL/Lo = - { 3.63E+00 * (D[xF]/sigx*)**2 + 1.78E+00 * (D[xD]/sigx*)**2
                          -  5.08E+00 * D[xF]*D[xD]/(sigx*)**2

               3.80E-06 * (S[xF]/sigx*)**2 + 1.24E-06 * (S[xD]/sigx*)**2
                          -  4.33E-06 * S[xF]*S[xD]/(sigx*)**2

               1.85E-01 * (D[yF]/sigy*)**2 + 8.49E-01 * (D[yD]/sigy*)**2
                          -  7.94E-01 * D[yF]*D[yD]/(sigy*)**2

               1.42E-08 * (S[yF]/sigy*)**2 + 3.11E-07 * (S[yD]/sigy*)**2
                          - -1.27E-07 * S[yF]*S[yD]/(sigy*)**2 }

                               **********

    with
          D[xF] = dx1_QF - dx2_QF , D[yF] = dy1_QF - dy2_QF
          D[xD] = dx1_QD - dx2_QD , D[yD] = dy1_QD - dy2_QD
          S[xF] = dx1_QF + dx2_QF , S[yF] = dy1_QF + dy2_QF
          S[xD] = dx1_QD + dx2_QD , S[yD] = dy1_QD + dy2_QD
```

```
*****************************************************************************
*                                                                           *
*                RELATIVE LUMINOSITY LOSS : KICKER CORRECTION               *
*                                                                           *
*****************************************************************************

   Random & uncorrelated quad motion (without last doublet)

   dL/Lo = - { 4.28E-03 * (sigx_QS/sigx*)**2
             + 2.75E-04 * (sigy_QS/sigy*)**2 }

   Fixed motion of the last doublet:

   dL/Lo = - { 3.41E-07 * (D[xF]/sigx*)**2 + 2.10E-08 * (D[xD]/sigx*)**2
                        -  1.69E-07 * D[xF]*D[xD]/(sigx*)**2

               3.50E-06 * (S[xF]/sigx*)**2 + 1.08E-06 * (S[xD]/sigx*)**2
                        -  3.88E-06 * S[xF]*S[xD]/(sigx*)**2

               1.79E-07 * (D[yF]/sigy*)**2 + 1.26E-08 * (D[yD]/sigy*)**2
                        -  9.49E-08 * D[yF]*D[yD]/(sigy*)**2

               1.40E-08 * (S[yF]/sigy*)**2 + 3.11E-07 * (S[yD]/sigy*)**2
                        - -1.32E-07 * S[yF]*S[yD]/(sigy*)**2 }


*****************************************************************************
*                                                                           *
*                          END OF PROGRAM LUM_LOSS                          *
*                                                                           *
*****************************************************************************
```